EPJ Web of Conferences **340**, 04010 (2025) https://doi.org/10.1051/epjconf/202534004010
Powders & Grains 2025

Packing behavior of cohesive deformable grains

Saeid Nezamabadi[1,2,3,*], *Farhang* Radjai[1], *Serge* Mora[1], *Jean-Yves* Delenne[2], *Ali* Hassanpour[3], and *Mojtaba* Ghadiri[3]

[1]LMGC, CNRS, Univ. Montpellier, 34090 Montpellier, France
[2]IATE, CIRAD, INRAE, Montpellier SupAgro, Univ. Montpellier, F-34060, Montpellier, France
[3]School of Chemical and Process Engineering, University of Leeds, Leeds LS2 9JT, UK

Abstract. Soft highly deformable particles are commonly found in biomass and industrial bio-products. Unlike most mineral grains, these particles exhibit significant deformation and shape changes even under moderate stress levels. In this study, we employ a continuum-discrete numerical approach to investigate the mechanical behavior of packings composed of cohesive soft disks. Our analysis includes the coordination number and particle shape evolution, the latter being quantified by a parameter that measures deviation from a circular shape. We find that during uniaxial compression of a packing initially composed of circular particles, the packing fraction at the jamming point, the coordination number and the shape parameter all increase with surface energy. During decompression, the combined effects of particle deformability and adhesion result in residual stresses and non-circular particle geometries. Both in loading and unloading, we observe a transition between a regime dominated by external stress and one dominated by internal cohesive stress.

1 Introduction

Many materials are composed of a disordered assembly of deformable particles, a characteristic commonly found in substances such as food powders, metal particles, colloidal suspensions, and clays. Unlike rigid particles, soft particles exhibit complex interactions due to their ability to undergo significant shape and volume changes, even under low confining pressures, forming extended contact areas when compressed. This property allows packings of deformable particles to achieve packing fractions that exceed those of rigid particles. Consequently, properties such as compressibility, shear strength, and microstructural attributes are governed by a combination of particle rearrangements as well as changes in particle shape and volume [1–7]. The variations in microstructure depend principally on the intrinsic characteristics of particles (such as compressibility and plasticity) and the interaction forces (such as friction and cohesion) between them. The interplay between particle deformation and adhesive forces plays a fundamental and critical role in determining the cohesive strength of granular materials.

In this paper, we employ numerical simulations to explore the combined effects of particle deformability and cohesion on key packing characteristics such as packing fraction, coordination number, particle deformation under stress, and force transmission within granular assemblies.

2 Methodology

The numerical approach uses an explicit total Lagrangian formulation of the Material Point Method (TLMPM) for computing particle deformations coupled with the Contact Dynamics (CD) method for modeling inter-particle interactions [8]. The TLMPM-CD technique enables a detailed analysis of the compaction behavior of elasto-plastic particle assemblies, with particular emphasis on behavior beyond the jamming state as influenced by material parameters and cohesion.

To characterize cohesion based on the particles' size and mechanical properties, a dimensionless number is defined as the ratio of the particle's cohesive energy to its elastic deformation energy: $C \propto \frac{U_C}{U_D}$. The particle cohesion energy is $U_C = \gamma\, S_c$, where γ is the surface energy and S_c denotes the contact surface area. Similarly, the particle deformation elastic energy is $U_D = \frac{1}{2} V_p \sigma_p \varepsilon_p = \frac{1}{2} V_p E \varepsilon_p^2$, where V_p, σ_p, ε_p, and E are the particle volume, stress, strain, and Young's modulus, respectively. By neglecting the strain ε_p as a dimensionless variable and considering two-dimensional simulations where $V_p \propto R^2$ and $S_c \propto R$ (R being the particle radius), we define a dimensionless *elasto-adhesion* number [9] as

$$C = \frac{\gamma}{ER}\,. \quad (1)$$

We investigate the uni-axial compression and decompression of 1000 elastic disks (particles) placed in a rectangular rigid box using our approach, as depicted in Figure 1(a). The diameters of the particles are uniformly distributed within the range $D \in [1.5, 2]$ mm. The initial configuration is carried out using CD simulations. To simulate the uni-axial compression, the top wall is moved downward at a constant velocity of $v_i = 0.02$ m/s with a time step $\Delta t = 10^{-4}$ ms. We then apply decompression to the packings by moving the top wall upward with the same velocity from a packing fraction of $\Phi = 0.9$ ($\Phi = V_S/V$,

*e-mail: saeid.nezamabadi@umontpellier.fr

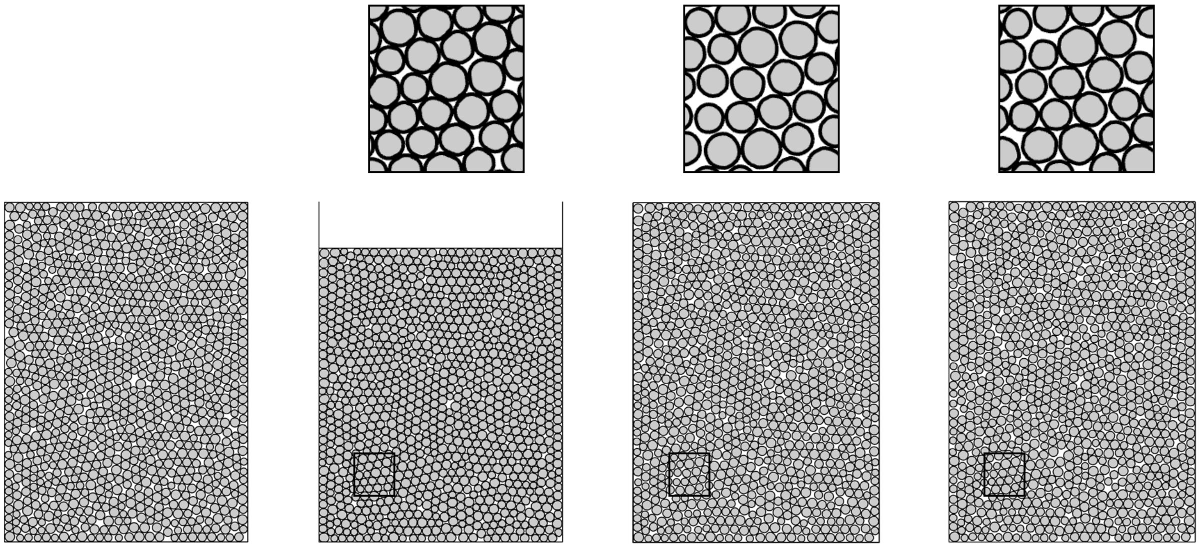

(a) Initial state: $\Phi = 0.80$ (b) $C = 0$ - $\Phi = 0.90$ (c) $C = 0$ - $\Phi = 0.80$ (d) $C = 0.069$ - $\Phi = 0.80$

Figure 1: Snapshots showing: (a) the initial configuration of an assembly of 1000 particles; (b) the compacted state at $C = 0$ and $\Phi = 0.90$; and (c–d) decompacted states at $\Phi = 0.80$ for $C = 0$ and $C = 0.069$. Zoomed views of the particles are also shown for snapshots (b-d).

where V_S is the volume of particles and V is the total volume).

In our simulations, we set the density of the particles $\rho = 1000$ kg/m^3, Young's modulus $E = 10$ kPa, and Poisson's ratio $\nu = 0.49$. A friction coefficient of $\mu_s = 0.5$ is considered between the particles, while there is no friction between the walls and the particles. To apply cohesion between the particles, five different cohesive surface energies are considered: $\gamma = 0$, 0.02, 0.2, 0.4 and 0.6 J/m^2. Therefore, considering Eq. (1), the values of the elasto-adhesion number are: $C = 0$, 0.002, 0.023, 0.046 and 0.069. Moreover, since the contact interactions are computed between material points [8], for each contact point, a cohesive force is defined as: $f_c = \gamma\, \delta x$, where δx is the mean distance between material points. The simulations are conducted under plane stress conditions with a relative spatial resolution of $\frac{\delta x}{\langle D \rangle} = 0.08$.

3 Results and discussion

Figure 1 shows snapshots of the samples, during compression and decompression. We see that the particle shapes deviate from circular to nearly polygonal, and the resulting particle deformations cause a decrease in the pore size between the particles (Fig. 1(b)). By decompressing the assembly, non-cohesive particles separate and almost return to their initial shape (Fig. 1(c)), while some cohesive particles form clusters and keep their deformed shape (Fig. 1(d)).

In Fig.2(a), the vertical stress σ is shown as a function of the packing fraction Φ for various values of the elasto-adhesion number C. For each value of C, σ initially fluctuates near zero up to a threshold in Φ, indicating the onset of collective jamming. To identify this jamming transition, we analyze the evolution of the mean incremental particle displacement in the y-direction, $\overline{\mathrm{d}Y}_p$, as illustrated in Fig.2(b) [8]. At a specific packing fraction $\Phi = \Phi_j$, the ratio $\overline{\mathrm{d}Y}p/\mathrm{d}Y_{\text{top wall}}$ abruptly drops below 0.5 and, for higher values of Φ, fluctuates around 0.5. This marks the transition to a jammed state. We observe that the jamming point shifts to higher Φ values as C increases, as shown in the inset of Fig. 2. This delay can be attributed to the fact that, although the particle-wall contacts are non-cohesive, the downward motion of the top wall activates cohesive interactions between particles, which hinders particle percolation through the box and delays the formation of a jammed structure. Beyond the jamming point, σ increases significantly. At high deformations, the remaining voids can only be eliminated through particle shape changes under elevated stress. Notably, for the same packing fraction Φ, a smaller stress σ is required as C increases.

To characterize the micro-structural evolution of the assemblies, the coordination number Z and a particle shape parameter $\mathcal{S}$ are considered. The parameter $\mathcal{S}$ is used to measure particle shape divergence from a circular shape and is defined as:

$$\mathcal{S} = 1 - \left\langle \frac{4\pi\mathcal{A}}{\mathcal{P}^2} \right\rangle, \tag{2}$$

where $\mathcal{P}$ and $\mathcal{A}$ are the perimeter and surface area of the particles, respectively. $\mathcal{S}$ is zero for a perfect disk and it increases toward 1 as the shape deviates from a circular shape. Figure 3 shows Z and $\mathcal{S}$ as a function of σ for different values of C. In Fig. 3(a), Z initially rises sharply to approximately 4 near the jamming point, regardless of C, when σ is very small. We observe that for all samples of

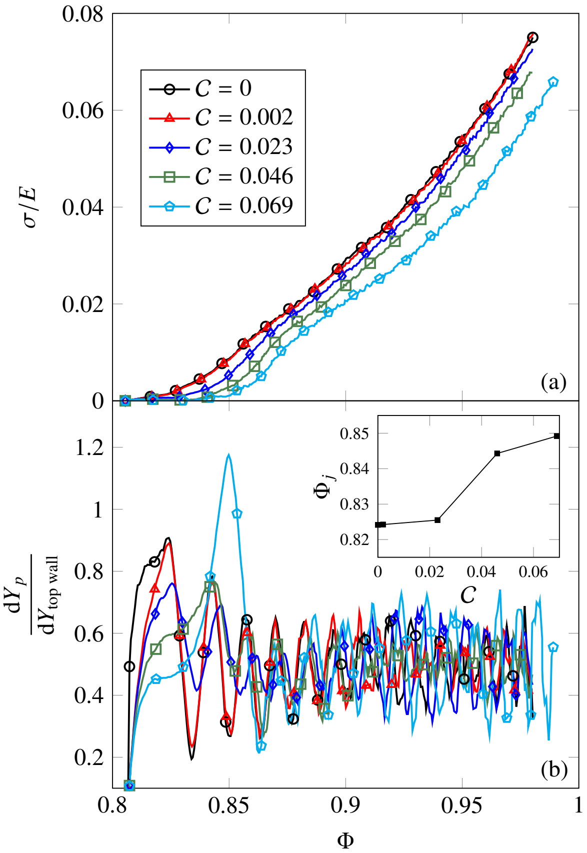

Figure 2: Vertical stress applied by the assembly to the bottom wall, σ, normalized by the particle Young's modulus E (a), and ratio of the mean incremental particle displacement to the top wall displacement in y-direction $\overline{\mathrm{d}Y_p}/\mathrm{d}Y_{\mathrm{top\ wall}}$ (b), as a function of packing fraction Φ for different values of the elasto-adhesion number C. Inset: Packing fraction at the jamming point Φ_j as a function of C.

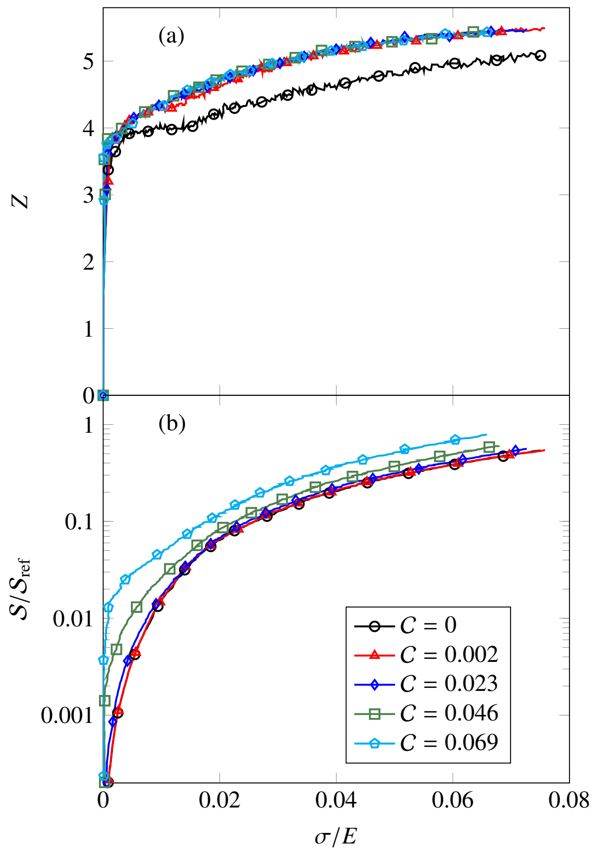

Figure 3: Coordination number Z (a) and particle shape parameter $\mathcal{S}$ (c) as a function of vertical stress σ.

nonzero C, the variations coincide and remain above that for $C = 0$.

Figure 3(b) shows $\mathcal{S}$, normalized by a reference value of particle shape parameter $\mathcal{S}_{\mathrm{ref}}$, as a function of σ. The reference value $\mathcal{S}_{\mathrm{ref}}$ corresponds to that of a regular hexagon and is given by $\mathcal{S}_{\mathrm{ref}} = 1 - \sqrt{3}\pi/6 \simeq 0.093$. For all values of C, $\mathcal{S}$ increases with σ, and this increase becomes more pronounced as C increases. This behavior is physically plausible since higher cohesion implies lower mobility of particles and thus the necessity of particle deformation to accommodate the imposed compressive strain. Furthermore, for small C values, particle shape begins to change at the jamming point Φ_j, while particle deformations are initiated before jamming for high C values. The normalized shape parameter increases toward 1, indicating that the particles tend to a nearly regular hexagonal shape.

Figure 4(a) displays the evolution of Z as a function of σ during loading and, unloading from $\Phi \simeq 0.9$ (*i. e.*, the packing started to unload at a packing fraction of $\Phi \simeq 0.9$). During the unloading, the coordination number Z decreases with decreasing σ. This reduction of Z occurs more slowly as the elasto-adhesion number C increases, and the final values of Z in fully unloaded samples are higher for larger C values (from $Z \simeq 1.42$ for $C = 0$ to $Z \simeq 2.37$ for $C = 0.069$).

Figure 4(b) shows the evolution of the normalized $\mathcal{S}$ as a function of σ during loading and unloading. During unloading, $\mathcal{S}$ declines with decreasing stress in all cases, but tends to increase in the most cohesive case ($C = 0.069$) while σ decreases. The residual value of $\mathcal{S}$ at the end of unloading increases with C, meaning that the particles keep their non-circular shape due to adhesion between particles. We see, however, that even cohesionless particles do not fully recover their initial circular shape due to the fact that in uniaxial compression elastic frictional particles can jam in a self-stressed configuration. This phenomenon is amplified by the finite lateral size of the system. The slight increase of $\mathcal{S}$ in the most cohesive cases can be attributed to transition from a regime governed by external load to a regime mainly governed by internal adhesion forces, which tend to deform the particles even in the absence of external forces.

4 Conclusions

In this paper, we employed a discrete-continuum approach to investigate the compaction behavior of deformable co-

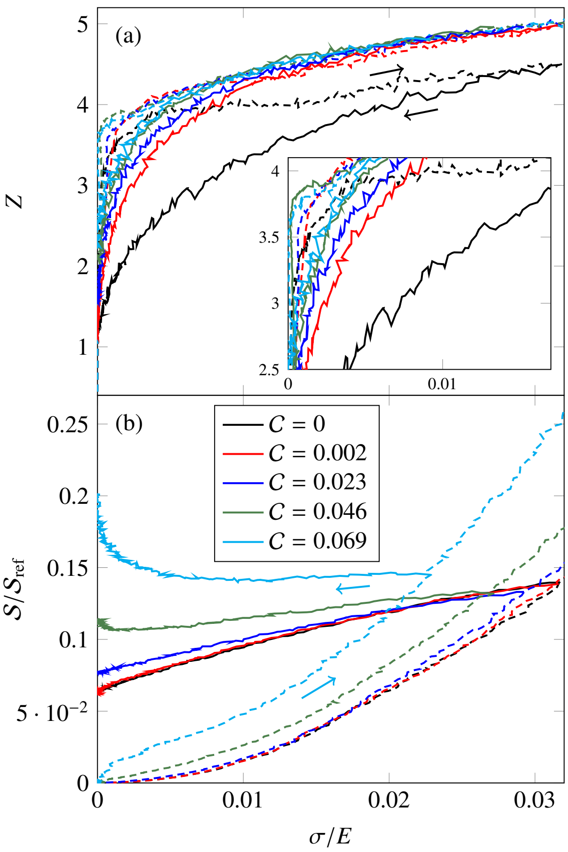

Figure 4: Coordination number Z (a) and particle shape parameter $\mathcal{S}$ (b) as a function of vertical stress σ during compressive loading (dashed line) and, unloading (solid line) from $\Phi \simeq 0.9$, for all values of the elasto-adhesion number C. Inset to (a): a zoom on the low σ part of the curves.

hesive granular systems. The TLMPM-CD method combines an explicit total Lagrangian formulation of the Material Point Method (TLMPM) with the Contact Dynamics (CD) approach to model inter-particle interactions. The adhesion between particles is modeled by attributing a surface energy to the particle surface. We studied the uniaxial compression and decompression for different values of surface energy.

In uniaxial compression of a packing of initially circular particles, the effect of surface energy appears through the increase of the jamming packing fraction and coordination number. We also defined a shape parameter that accounts for the degree of deviation from circular shape. This parameter increases during compression and the particles tend to regular hexagonal shapes. During decompression, while the applied stress declines toward zero, the particles partially keep their circular shapes due to the combination of deformability and adhesion. We observed a transition between a regime governed by external stress and a regime governed by internal cohesive stress. We have investigated the full scaling involving the external pressure, cohesive stress, elastic modulus, friction coefficient, and Poisson's ratio on the loading-unloading behavior, but the results will be published elsewhere.

The authors acknowledge the support of the French *Agence Nationale de la Recherche* (ANR), under grant ANR-20-CE08-0011 (PaMaCo project). We are also grateful to the Genotoul Bioinformatics platform Toulouse Occitanie (Bioinfo Genotoul, https://doi.org/10.15454/1.5572369328961167E12) for providing computing resources.

References

[1] R. Bonnecaze, M. Cloitre, Micromechanics of soft particle glasses, Advances in Polymer Science **236**, 117 (2010).

[2] M. van Hecke, Jamming of soft particles: geometry, mechanics, scaling and isostaticity, Journal of Physics: Condensed Matter **22**, 033101 (2010).

[3] G. Mollon, A multibody meshfree strategy for the simulation of highly deformable granular materials, International Journal for Numerical Methods in Engineering **108**, 1477 (2016).

[4] T.L. Vu, J. Barés, S. Mora, S. Nezamabadi, Numerical simulations of the compaction of assemblies of rubberlike particles: A quantitative comparison with experiments, Physical Review E **99**, 062903 (2019).

[5] S. Nezamabadi, X. Frank, J.Y. Delenne, J. Averseng, F. Radjai, Parallel implicit contact algorithm for soft particle systems, Computer Physics Communications **237**, 17 (2019).

[6] D. Cantor, M. Cárdenas-Barrantes, I. Preechawuttipong, M. Renouf, E. Azéma, Compaction model for highly deformable particle assemblies, Physical Review Letters **124**, 208003 (2020).

[7] J. Clemmer, J. Lechman, Onset and impact of plastic deformation in granular compaction, Powder Technology **452**, 120563 (2025).

[8] S. Nezamabadi, F. Radjai, Explicit total lagrangian material point method with implicit frictional-contact model for soft granular materials, Granular Matter **26**, 67 (2024).

[9] H. Fu, A. Crosby, Determining the elasto-adhesion length by void collapse in ultra-soft materials, Soft Matter **19**, 932 (2023).